

Spin switching in tris(8-Aminoquinoline)iron(II)(BPh₄)₂: quantitative guest-losing dependent spin crossover properties and single-crystal-to-single-crystal transformation

Feng-Lei Yang,^{*a,c} Xin Chen,^a Wen-Hao Wu,^a Jing-Hang Zhang,^a Xiang-Mei Zhao,^a Yan-Hui Shi^a and Fei Shen^{*b}

^aSchool of Chemistry and Material Science and Jiangsu Key Laboratory of Green Synthetic Chemistry for Functional Materials, Jiangsu Normal University, Xuzhou, Jiangsu 221116, P. R. China

E-mail: yangfl@jsnu.edu.cn.

^bCollege of Physical Education and Health & Education Ministry Key Laboratory of Adolescent Health Assessment and Exercise Intervention of Ministry of Education, East China Normal University, Shanghai 200241, P. R. China

E-mail: doctorfly@yeah.net.

^cState Key Laboratory of Physical Chemistry of Solid Surfaces and Department of Chemistry, College of Chemistry and Chemical Engineering, Xiamen University, Xiamen 361005, China

Table S1. Hydrogen bonding for compound **1•2CH₃CN** and **2•1.5CH₃COCH₃** [Å and °].

D-H...A	d(D-H)	d(H...A)	d(D...A)	∠(DHA)	Symmetry code
1•2MeCN					
N(3)-H(10C)...N(8) ^{#1}	0.91	2.45	3.198(9)	139.2	^{#1} x-1,y,z
C(64A)-H(64B)...N(8)	0.95	2.38	3.004(15)	123.3	
C(65A)-H(65B)...N(8)	0.95	2.5	3.057(16)	117.2	
2•1.5CH₃COCH₃					
N(3)-H(3A)…O(2)	0.92	2.02	2.938(6)	172.2	
C(2)-H(2A)…O(1)	0.95	2.43	3.1383	131	
C(8)-H(8A)…N(6)	0.95	2.55	3.0619	114	
C(114)-H(11G)…O(1)	0.95	2.45	3.2786	146	
C(17)-H(17A)…N(2)	0.95	2.58	3.0669	112	
C(26)-H(26A)…N(4)	0.95	2.53	3.0249	113	
C(97)-H(97A)…O(1)	0.95	2.39	3.2681	154	

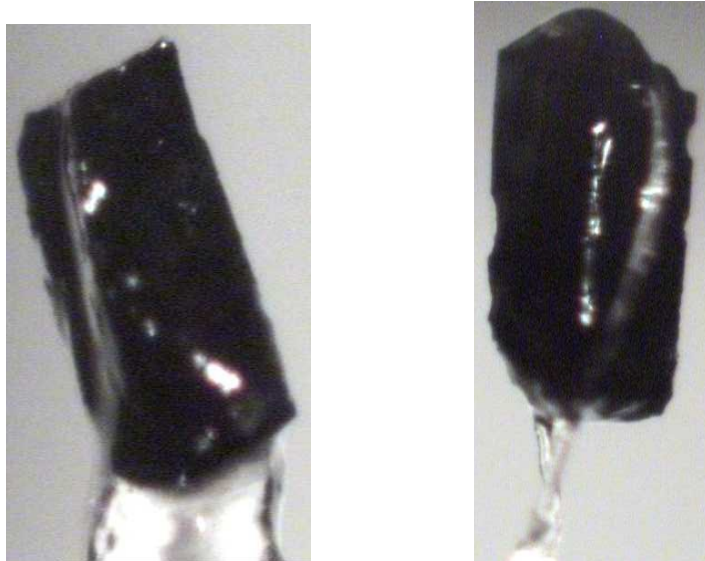


Fig. S1 The pictures for the crystals of compound **1•2CH₃CN** (left, before desolvation) and **1** (right, after desolvation).

Table S2. Crystallographic Data and Structure Refinement Details for Compound **1** at 120 and 300 K

1		
Formula	C ₇₅ H ₆₄ B ₂ FeN ₆	
F.W.	1126.8	
Crystal	Monoclinic	
Space group	<i>P</i> 2 ₁ /c	
<i>T</i> (K)	120(2)	300(20)
<i>a</i> (Å)	12.2941(4)	12.3622(6)
<i>b</i> (Å)	33.9568(11)	34.072(2)
<i>c</i> (Å)	19.0280(8)	19.1112(11)
α (deg)	90	90
β (deg)	129.852(3)	129.397(4)
γ (deg)	90	90
<i>V</i> (Å ³)	6098.3(5)	6220.6(7)
<i>Z</i>	4	4
<i>D</i> (g cm ⁻³)	1.227	1.203
μ (mm ⁻¹)	0.297	0.291
<i>F</i> (000)	2398	2368
RefIns obsd	9577	9092
<i>S</i>	1.199	1.146
<i>R</i> ₁	0.0956	0.0992
<i>wR</i> ₂	0.2231	0.1698

Table S3. Selected Bond Lengths [Å] and Angles [°] for Compounds **1** at 120 and 300 K

	1 -120K	1 -300K
Fe(1)-N(1)	1.942(4)	1.982(4)
Fe(1)-N(4)	1.971(4)	2.073(4)
Fe(1)-N(5)	1.967(4)	2.059(4)
Fe(1)-N(3)	2.029(4)	2.010(4)
Fe(1)-N(6)	2.021(4)	2.011(4)
Fe(1)-N(2)	2.057(4)	2.054(4)
N(1)-Fe(1)-N(4)	97.31(17)	N(1)-Fe(1)-N(2) 91.40(16)
N(1)-Fe(1)-N(5)	94.91(17)	N(1)-Fe(1)-N(3) 173.17(18)
N(4)-Fe(1)-N(5)	93.40(17)	N(1)-Fe(1)-N(4) 98.40(18)
N(5)-Fe(1)-N(3)	82.76(17)	N(1)-Fe(1)-N(5) 94.06(17)
N(1)-Fe(1)-N(6)	83.73(17)	N(1)-Fe(1)-N(6) 82.06(18)
N(3)-Fe(1)-N(2)	91.94(16)	N(3)-Fe(1)-N(2) 93.97(16)
N(6)-Fe(1)-N(2)	91.60(16)	N(4)-Fe(1)-N(2) 81.47(17)
N(5)-Fe(1)-N(6)	92.29(17)	N(4)-Fe(1)-N(3) 86.59(16)
N(3)-Fe(1)-N(6)	92.39(17)	N(4)-Fe(1)-N(5) 94.16(17)
N(1)-Fe(1)-N(2)	90.62(17)	N(4)-Fe(1)-N(6) 172.71(18)
N(4)-Fe(1)-N(2)	82.60(16)	N(5)-Fe(1)-N(2) 173.46(17)

N(4)-Fe(1)-N(3)	86.79(17)	N(5)-Fe(1)-N(3)	80.86(17)
<Fe-N> [Å]	1.998	2.032	
\sum [°]	48.58	58.91	
Θ [°]	224.077	229.009	
CShM's	0.415	0.619	
Octahedral volume [Å ³]	10.530	11.095	

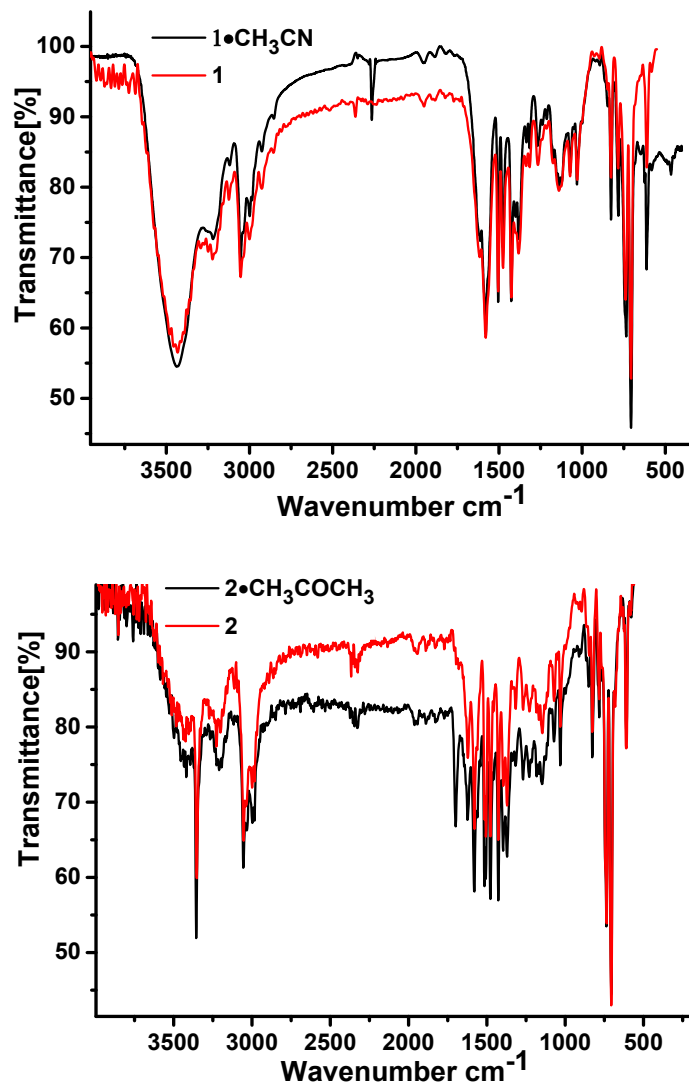


Fig. S2 The IR spectra of compound **1•2CH₃CN** and **1**(top), **1•1.5CH₃COCH₃** and **2** (bottom) at room temperature in the KBr pellets.

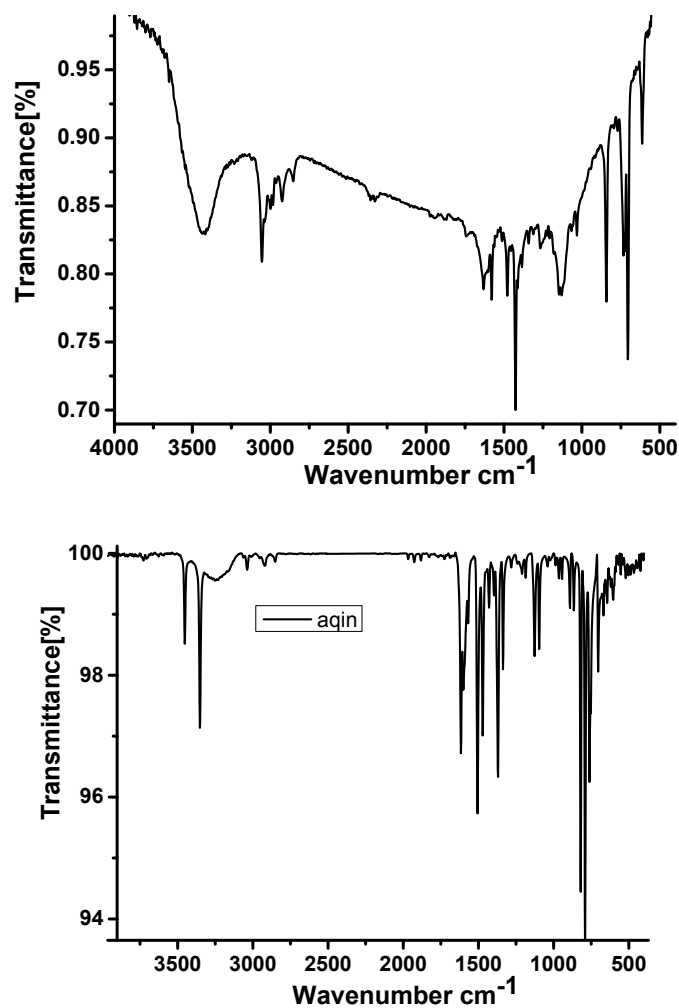


Fig. S3. The IR spectra of the magenta floccule (top) produced in the synthesis of the compounds and the aqin ligand (bottom) at room temperature.

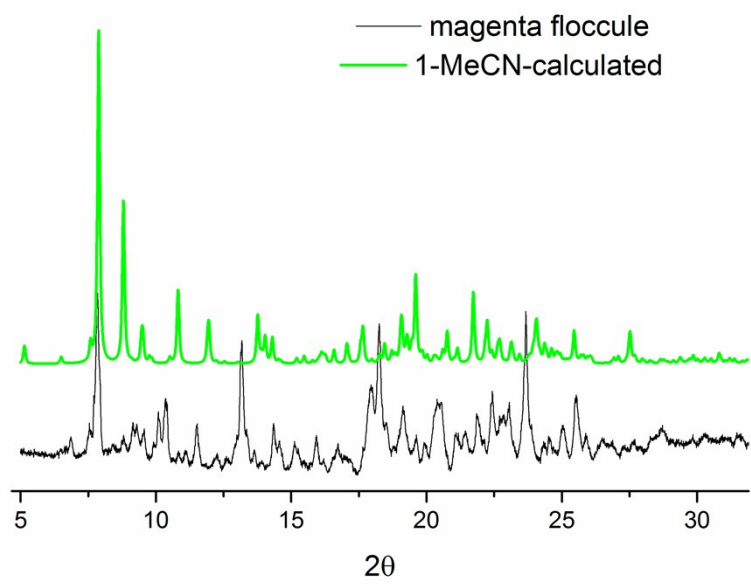


Fig. S4. The PXRD data suggests that the magenta floccule are not the target compound **1•2CH₃CN**.

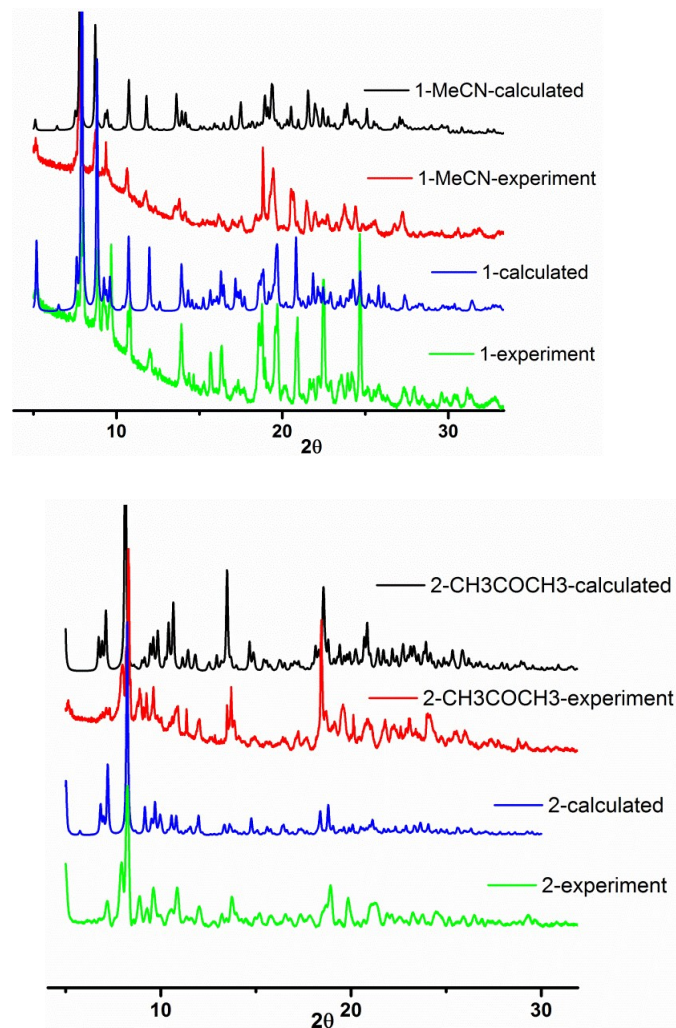


Fig. S5. The PXRD data of the samples of compound **1**• $2\text{CH}_3\text{CN}$ and **1** (top), **2**• $1.5\text{CH}_3\text{COCH}_3$ and **2** (bottom). The calculated data of **2** was obtained from the single-crystal data of **2**• $1.5\text{CH}_3\text{COCH}_3$ after the squeeze treatment by Platon.

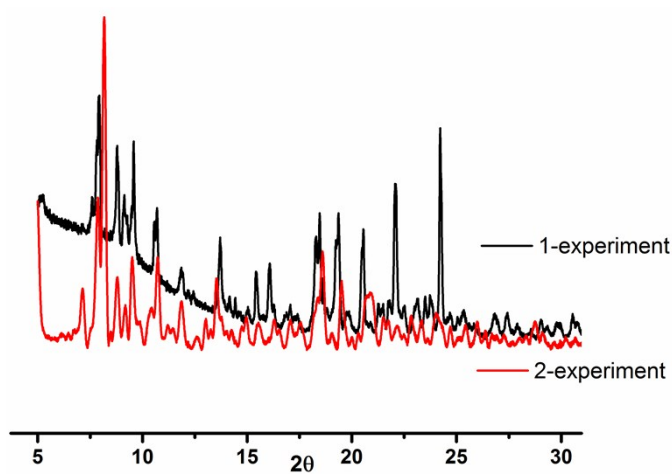


Fig. S6. The comparison of the XRD data between the samples of compound **1** and **2** suggests that they are not the same material.

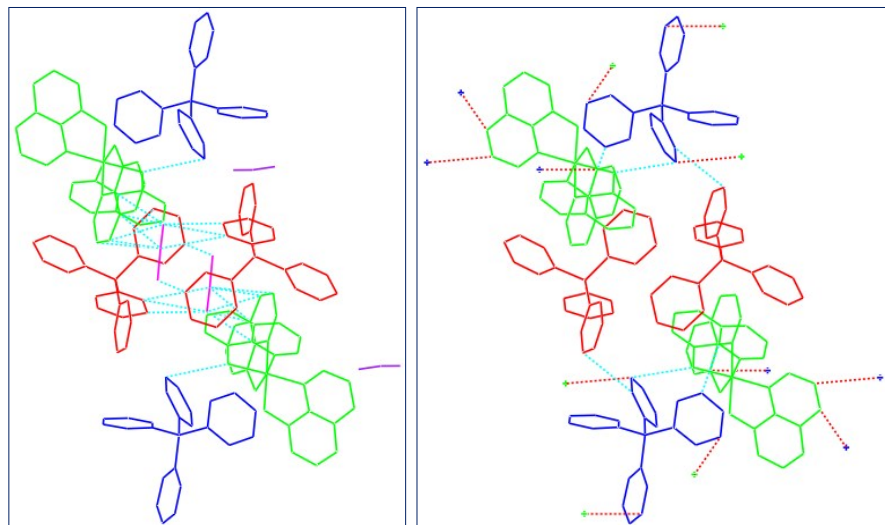


Fig. S7 The short contacts (shorter than the sum of vdw radii) for **1•2CH₃CN** (left) and **1** (right) calculated by Mercury software.

Green-[Fe(aqin)₃]²⁺, red and blue-BPh₄⁻, purple-CH₃CN, dashed line-short contacts.

Table S4. Analysis of short contacts Interactions (calculated by Mercury) for **1•2CH₃CN** and **1**.

Atom1	Atom2	Symmetrical code	distance [Å]	Atom1	Atom2	Symmetrical code	distance [Å]
1•2CH₃CN				1			
N3	C48	1+x,y,z	3.231	N3	C48	1+x,y,z	3.208
C53	C76	-1+x,y,z	3.318	C5	C36	1+x,y,z	3.336
C9	C55	2-x,-y,1-z	3.364	C18	C38	x,1/2-y,-1/2+z	3.397
C26	C77	x,y,z	3.189	C20	C30	x,1/2-y,-1/2+z	3.288
C24	C77	x,y,z	3.303	C47	C61	x,1/2-y,1/2+z	3.352
C64	C77	-1+x,y,z	3.378	C17	C48	x,y,z	3.388
C25	C77	x,y,z	3.021				
C25	N8	x,y,z	3.237				
N8	C64	1+x,y,z	3.229				
N8	C65	1+x,y,z	3.221				
C19	N8	x,y,z	3.104				
C24	N8	x,y,z	3.006				

Table S5. Analysis of X-H···Cg(π -Ring) Interactions (H···Cg < 3.0 Å, Gamma < 30.0°) calculated by Platon for **1•2CH₃CN** and **1**.

X--H(I) ··· Cg(J)	H···Cg [Å]	<X-H···Cg[°]	X···Cg[Å]	H···Cg[Å]	<X-H···Cg[°]	X···Cg[Å]
1•2CH₃CN				1		
N(3)-H(10D)···Cg(13) ^b	2.47	134	3.174	2.39	131	3.0943
N(6)-H(10F)···Cg(11) ^b	2.55	142	3.3075	2.5	143	3.3097
C(9)-H(9A)···Cg(14) ^a	2.46	137	3.2234	2.81	129	3.4793
C(9)-H(9A)···Cg(14A) ^a	2.83	134	3.5584			
C(25)-H(25A)···Cg(16) ^d	2.79	161	3.7012	2.67	161	3.5817
C(25)-H(25A)···Cg(16 A) ^d	2.63	165	3.5558			
C(29)-H(29A)···Cg(4) ^c	2.93	150	3.7798	2.82	153	3.693
C(40)-H(40A)···Cg(8)	2.91	129	3.5821	2.85	133	3.5769
C(43)-H(43A)···Cg(8)	2.88	143	3.6822	3.00	140	3.7783
C(23)-H(23A) ··· Cg(14A) ^d	2.9	141	3.6916			
C(77)-N(8)···Cg(5) ^e	2.945	93	3.2035			
C(79)-H(79C)···Cg(10)	2.89	115	3.4138			
C(3)-H(3A)···Cg(17)				2.96	161	3.8612
N(3)-H(10C)···Cg(13)				2.39	131	3.0943
C(18)-H(18A)···Cg(13)				2.95	134	3.6697
C(26)-H(26A)···Cg(17)				2.99	141	3.7711
C(60)-H(60A)··· Cg(12)				2.93	139	3.6904

Symmetry code: ^a 2-X, -Y, 1-Z; ^b 1+X, Y, Z; ^c X, 1/2-Y, 1/2+Z; ^d 1-X, -Y, -Z; ^e -1+X, Y, Z

The constituent of ring Cg(J):

Cg(4): N(1)C(15)C(14)C(18)C(17)C(16); Cg(5): N(4)C(19)C(24)C(25)C(26)C(27); Cg(8): C(10)C(11)C(12)C(13)C(14)C(15);
 Cg (10): C(28)C(29)C(30)C(31)C(32)C(33); Cg(11): C(34)C(35)C(36)C(37)C(38)C(39); Cg(13): C(46)C(47)C(48)C(49)C(50)C(51);
 Cg(14): C(52)C(53)C(54)C(55)C(56)C(57); Cg(14A): C(52A)C(53A)C(54A)C(55A)C(56A)C(57A);
 Cg (15): C(40)C(41)C(42)C(43)C(44)C(45); Cg(16): C(64)C(65)C(66)C(67)C(68)C(69);
 Cg(16A): C(64A)C(65A)C(66A)C(67A)C(68A)C(69A); Cg(17): C(70)C(71)C(72)C(73)C(74)C(75)

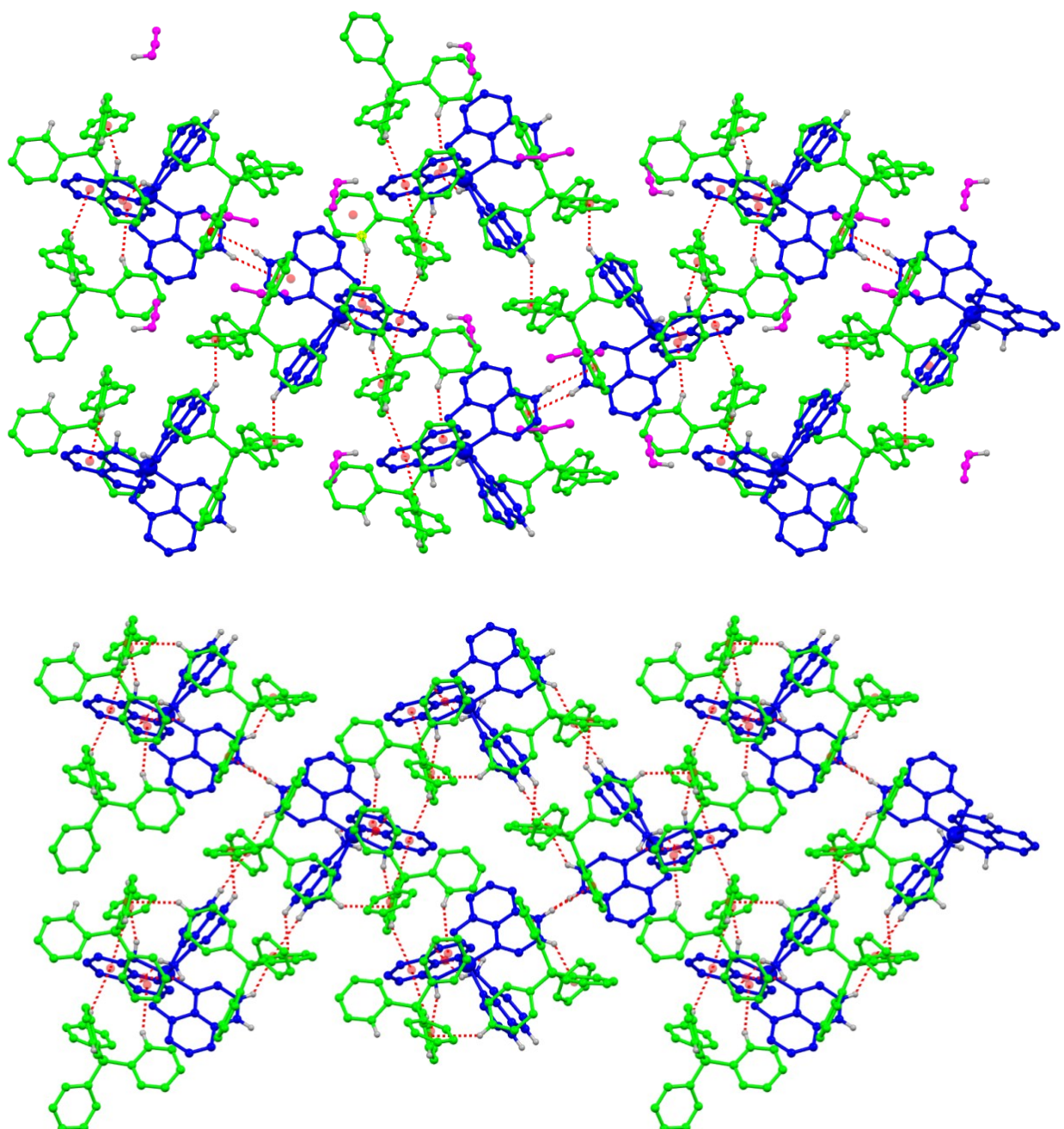


Fig. S8 The obviously varied C-H···Cg like intermolecular contacts (calculated by Platon software) in the **1•2CH₃CN** (top) comparing with **1**(bottom), blue-[Fe(aqin)₃]²⁺, green-BPh₄⁻, purple-CH₃CN, red ball- centres of the aromatic rings, red dashed line- X-H···Cg contacts, gray ball-involved hydrogen atoms. The uninvolved hydrogen atoms were omitted for clarity.

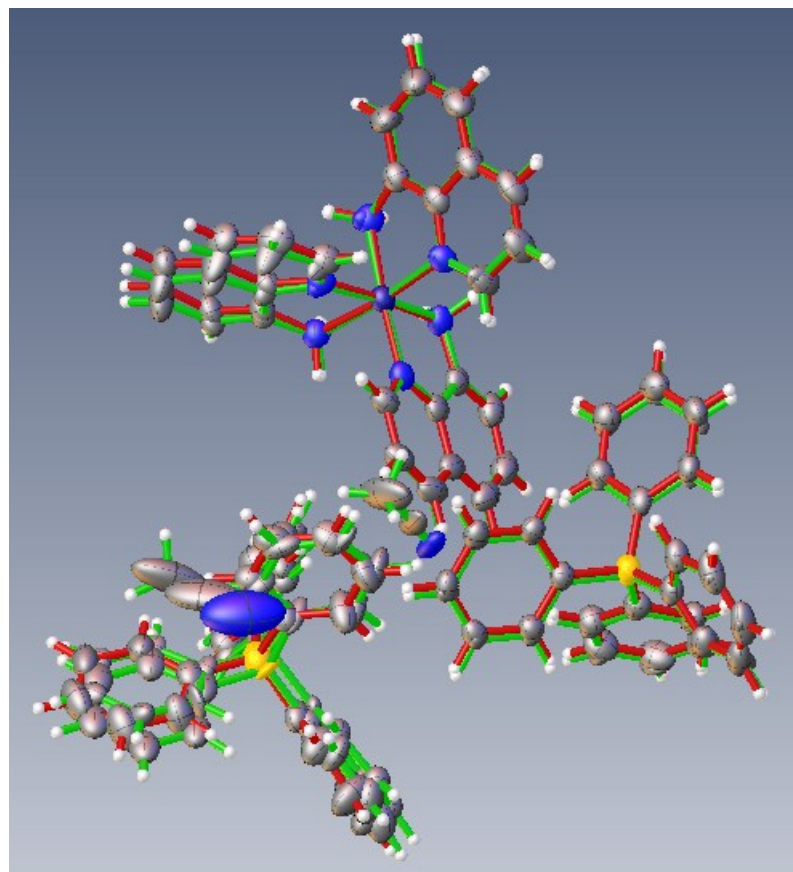


Fig. S9 The overlay of molecules between **1•2CH₃CN** (bond in green) and **1**(bond in red).

Table S6 For **1•2CH₃CN** with the solvent removed, PLATON gives the voids thus:

For desolvated **1** (at 173K, but similarly at 120 and 300K):

```

loop_
    _platon_squeeze_void_nr
    _platon_squeeze_void_average_x
    _platon_squeeze_void_average_y
    _platon_squeeze_void_average_z
    _platon_squeeze_void_volume
    _platon_squeeze_void_count_electrons
    _platon_squeeze_void_content

```

1	0.442	0.141	0.708	97	5 ''
2	0.442	0.358	0.208	98	5 ''
3	0.400	0.040	0.305	11	0 ''
4	0.400	0.460	0.805	11	0 ''
5	0.558	0.641	0.792	97	5 ''
6	0.558	0.858	0.292	98	5 ''
7	0.502	0.500	1.004	41	-1 ''
8	0.502	0.999	0.504	41	-1 ''
9	0.602	0.543	0.200	10	0 '

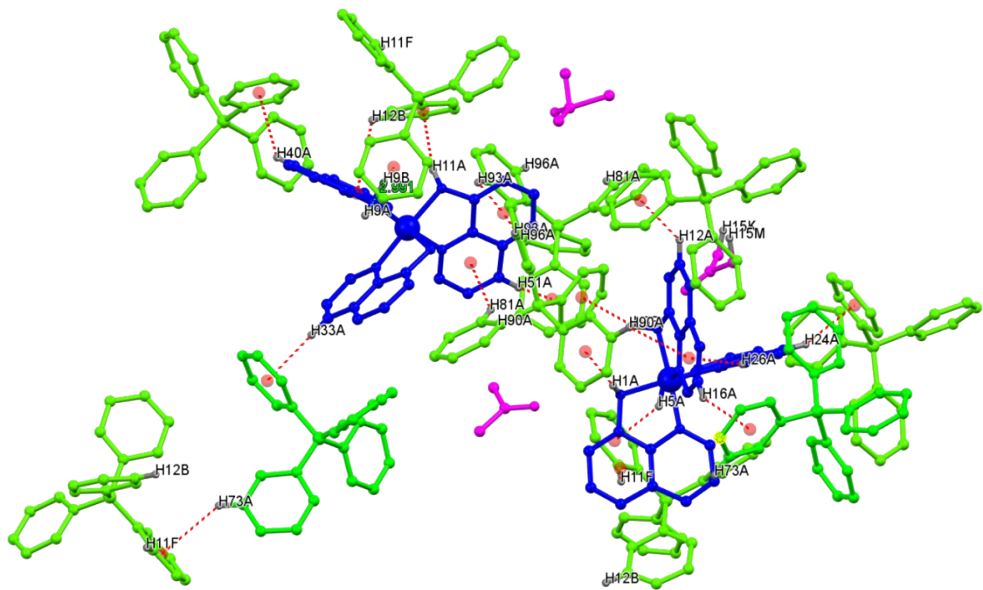


Fig. S10 The C-H···Cg intermolecular contacts (calculated by Platon software) in the **2•1.5CH₃COCH₃**, blue-[Fe(aqin)₃]²⁺, green-BPh₄⁻, purple-CH₃COCH₃, red ball- centres of the aromatic rings, red dashed line- X-H···Cg contacts, gray ball-involved hydrogen atoms. The uninvolved hydrogen atoms were omitted for clarity.

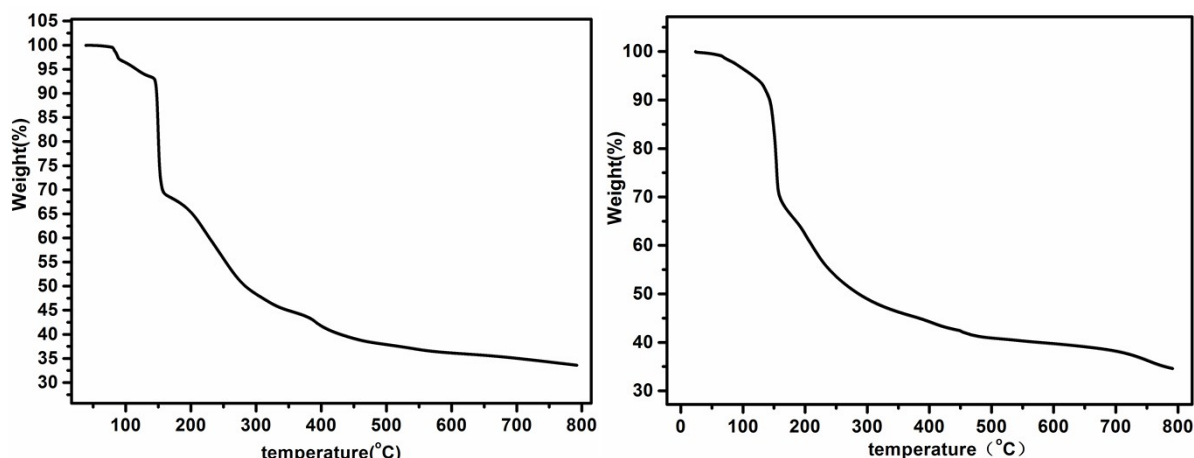


Fig. S11 The TGA of compound **1•2CH₃CN** (right) and **1•1.5CH₃COCH₃** (left)

Table S8. Parameters of Mössbauer spectra for **1•2CH₃CN** and **1** at room temperature (293 K). ^a

Compound	δ [mm/s]	ΔE_Q [mm/s]	Γ [mm/s]	Relative area[%]	States
1•2CH₃CN					
	0.116		0.582	100	LS
1	0.835	2.870	0.481	41.1	HS
	0.157		0.582	58.9	LS

^a δ : isomer shift (with reference to metallic iron at 293 K), ΔE_Q : quadrupole splitting, Γ : half-height width.

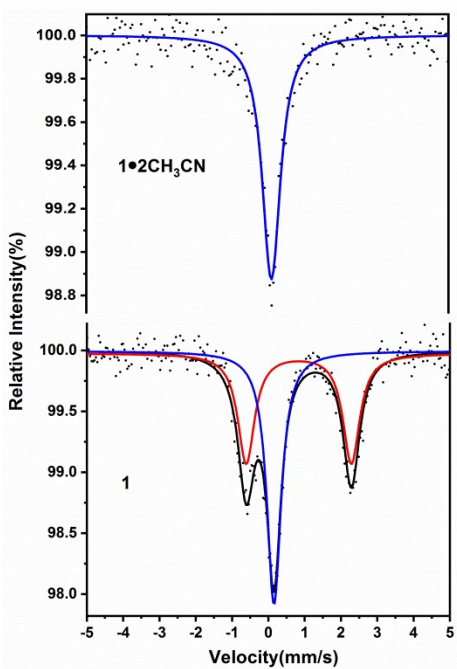


Fig. S12 The Mössbauer Spectra for complex **1**•2CH₃CN and the desolvated compound **1** at room temperature (293 K).

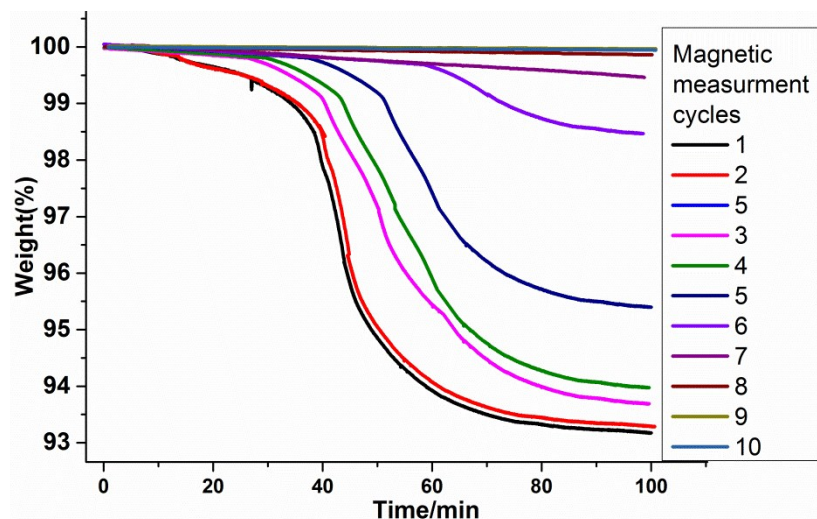


Fig. S13. The TGA analyses of compound **1**•2CH₃CN in each cycle of magnetic measurements.

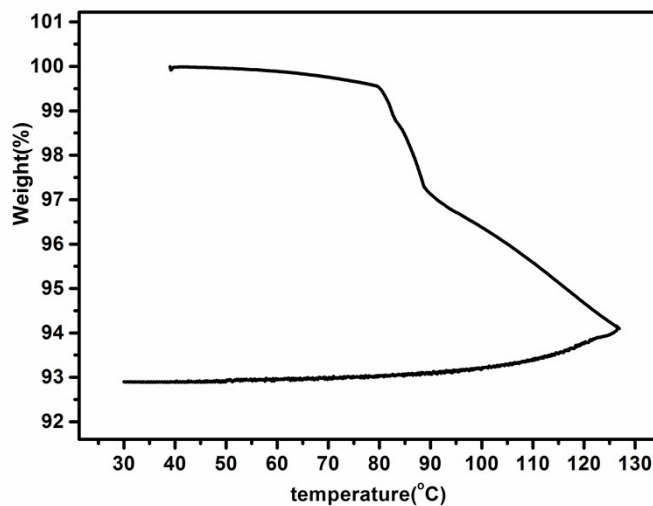


Fig. S14. The TGA of compound **1•2CH₃CN** upon cooling to room temperature after heated to 400 K.

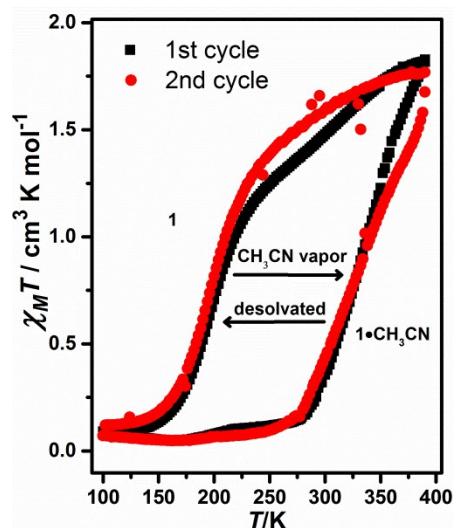


Fig. S15 Plots of the $\chi_M T$ vs T for complex **1•2CH₃CN** and the desolvated compound **1** with a scan rate of 1 K min⁻¹ in two different heating and cooling cycles. The process is: from 100→390 as **1•2CH₃CN** is heated at 390 K for two hours to give **1** then from 390→100 K, taking the sample from the magnetometer to be exposed to CH₃CN vapour for 2 hours to regenerate **1•2CH₃CN**, then starting the second 100→390→100 K cycle.